

See discussions, stats, and author profiles for this publication at: <https://www.researchgate.net/publication/264167247>

Chain-Growth Insertion Polymerization of 1,3-Diethynylbenzene High Internal Phase Emulsions into Reactive π-Conjugated Foams

ARTICLE *in* MACROMOLECULES · JULY 2014

Impact Factor: 5.8 · DOI: 10.1021/ma501142d

CITATIONS

6

READS

41

7 AUTHORS, INCLUDING:



Jirí Zedník

Charles University in Prague

41 PUBLICATIONS 410 CITATIONS

[SEE PROFILE](#)



Sebastijan Kovačič

National Institute of Chemistry

21 PUBLICATIONS 268 CITATIONS

[SEE PROFILE](#)

Chain-Growth Insertion Polymerization of 1,3-Diethynylbenzene High Internal Phase Emulsions into Reactive π -Conjugated Foams

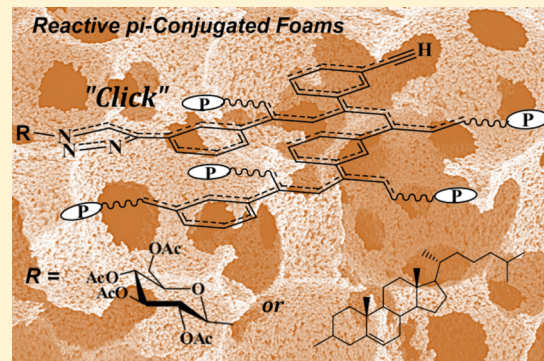
Eva Slováková,[†] Marjan Ješelník,[‡] Ema Žagar,[‡] Jiří Zedník,[†] Jan Sedláček,^{*,†} and Sebastijan Kovačič^{*,‡}

[†]Department of Physical and Macromolecular Chemistry, Faculty of Science, Charles University in Prague, Hlavova 9, 128 43 Praha 2, Czech Republic

[‡]Laboratory for Polymer Chemistry and Technology, National Institute of Chemistry, Hajdrihova 19, 1000 Ljubljana, Slovenia

S Supporting Information

ABSTRACT: The π -conjugated micro/macroporous polyacetylene-type polyHIPE foams were synthesized for the first time by a chain-growth insertion polymerization of high internal phase emulsions (HIPEs). In the first step, the π -conjugated polyHIPE foams were prepared by polymerization of 1,3-diethynylbenzene HIPEs using $[\text{Rh}(\text{nbd})\text{acac}]$ complex as a catalyst. The π -conjugated polyHIPE foams consist of ethynylphenyl-substituted polyene main chains which are cross-linked by the 1,3-phenylene linkers. In the second step, the foams were chemically and thermally postmodified by applying the alkyne–azide cycloaddition reaction and the solvent free solid phase hyper-cross-linking at temperature of 280 °C. Thus, obtained polyacetylene-type polyHIPE foams exhibit hierarchically structured micro/macroporous morphology with sizes of the macropores and interconnecting pores of $3.4 \pm 0.3 \mu\text{m}$ (or $4.8 \pm 0.8 \mu\text{m}$) and $0.96 \mu\text{m}$ (or $1.1 \mu\text{m}$), respectively, wherein a substantial volume of micropores is also found within the macroporous walls as revealed by the calculations from the *t*-plots. The BET (Brunauer–Emmett–Teller) surface area of up to 110 and $380 \text{ m}^2 \text{ g}^{-1}$ was determined before and after solid phase hyper-cross-linking, respectively.



INTRODUCTION

The chain growth polymerization of ethynyl-containing monomers with transition-metal catalysts produces substituted polyacetylenes, i.e., conjugated polymers with alternating double and single bonds along the main chains.¹ This unique electronic structure endows substituted polyacetylenes with the properties (e.g., optical, magnetic, and luminescence properties),² which are very difficult to access with the corresponding vinyl polymers. Recently, the π -conjugated microporous polymers (CMPs)³ have been attracted much attention owing to the high specific surface area, high extent of π -conjugation as well as pronounced and tunable microporosity. These materials have been widely studied in many application fields like gas separation,⁴ reversible storage,⁵ heterogeneous catalysis,⁶ optoelectronics, and sensors.⁷ Various step-growth polymerizations based on coupling and condensation reactions have been used for the CMPs preparation.³ Recently, the chain-growth polymerization of ethynyl-containing monomers has been demonstrated to be an effective tool for the CMPs preparation.⁸ The major drawback of all microporous materials (including CMPs) and with this associated limited practical use of these materials is that they suffer from slow kinetics due to the mass transport limitations. Therefore, combining high surface area of CMPs with macroporous architecture of, e.g., polyHIPEs⁹ (*vide infra*) would greatly improve the hydrodynamic properties of CMPs and open up new application opportunities of such systems.

High internal phase emulsions (HIPEs), yielding the polyHIPEs after polymerization, are heterogeneous liquid–liquid mixtures characterized by a droplet (internal) phase volume fraction of at least 74% of the total emulsion volume.¹⁰ Templating within the high internal phase emulsions (HIPEs) represents an interesting technique for the production of macroporous polymeric materials and has become very active research area.¹¹ Several polymerization mechanisms like free radical polymerization (FRP),¹² ATRP,¹³ RAFT,¹⁴ thiol–ene, and thiol–yne reactions,¹⁵ as well as ROMP,¹⁶ have been already used to solidify HIPEs. Recently, Zhang et al. reported the use of HIPE templating approach to combine the properties of polyHIPEs and CMPs, but the cavity-like structure of polyHIPEs and the high specific surface area of CMPs, representing the typical characteristics of these two types of materials, are missing. Nevertheless, thus obtained π -conjugated polyHIPEs were successfully applied as the heterogeneous photocatalysts.¹⁷

Herein, we propose for the first time rhodium catalyzed chain-growth insertion polymerization as a new tool for the preparation of reactive and well-defined three-dimensional (3D) micro/macroporous π -conjugated polyHIPE foams from the 1,3-diethynylbenzene (1,3-DEB) high internal phase

Received: June 2, 2014

Revised: July 17, 2014

Published: July 24, 2014

emulsions (HIPE). Furthermore, a potential of postmodification of nonreacted ethynyl groups either chemically via the azide “click” reaction or thermally via the aromatization reaction, is demonstrated.

EXPERIMENTAL SECTION

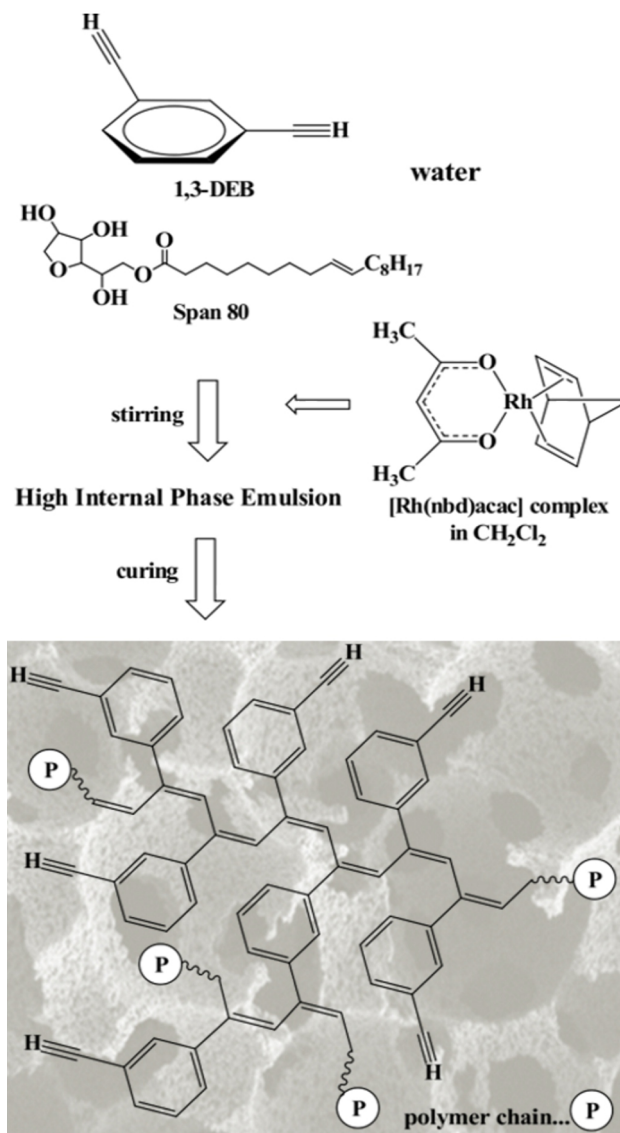
Materials and Synthesis. 1,3-Diethynylbenzene (1,3-DEB) (TCI Europe; amounts according to Table S1, Supporting Information) and surfactant Span80 (Sorbitan monooleate; MW = 428 g·mol⁻¹; Sigma-Aldrich) were placed in a 50 mL ampule and the mixture was stirred with an overhead stirrer at 400 rpm. The corresponding amount (*cf.* Table S1) of deionized water was added dropwise under constant stirring. After addition of water the mixture was further stirred for 1 h until a uniform emulsion was formed. Then, a solution of the catalyst (acetylacetone)(bicyclo[2.2.1]hepta-2,5-diene)rhodium(I), [Rh-(nbd)acac] (Sigma-Aldrich; *cf.* Table S1) in dichloromethane (Lachema, Czech Republic) was added to the emulsion and the mixture was further stirred for 1 min. Subsequently, the emulsion was cured at room temperature for 3 h. The resulting solid polymer, poly(1,3-DEB), was repeatedly washed with CH₂Cl₂, separated by filtration, and dried in a vacuum oven at room temperature.

Characterization. The morphology investigations were performed by a scanning electron microscopy (SEM). The SEM images were taken on a Field emission electron microscope Ultra+ (Carl Zeiss) equipped with an energy dispersive spectrometer SDD X-Max 50 (Oxford Instruments). A piece of each sample was mounted on a carbon tab for better conductivity and the thin layer of gold was sputtered on the sample’s surface prior scanning analysis (See details in the Supporting Information). The nitrogen adsorption measurements of polymer samples were performed on a Micromeritics TriStar 3000 surface area analyzer. The samples were outgassed at 90 °C under turbomolecular vacuum pump. The BET surface area was determined by means of nitrogen adsorption data in a relative pressure range from 0.05 to 0.25. In this pressure range the BET transform plots were linear. The ¹³C CP/MAS NMR spectra were measured at 11.7 T using a Bruker Avance 500 WB/US NMR spectrometer with a double-resonance 4 mm probe head at a spinning frequency of 20 kHz. The Fourier transform IR (FTIR) spectra were measured on a Nicolet Magna IR 760 using the diffuse reflection mode (DRIFTS). Samples were diluted with KBr. The diffuse reflectance UV-vis (DR UV-vis) spectra of the solid polymers were recorded on a Perkin–Elmer Lambda 950 spectrometer. The polymers were diluted with BaSO₄ (1/10, w/w) before the measurements. The photoluminescence (PL) emission spectra of the solid polymers were measured on a Horiba Jobin Yvon Fluorolog 3 using a solid-state film holder (22.5 deg angle) and an excitation wavelength of 420 nm. Samples for the measurements were prepared as follows. Approximately 10 mg of finely powdered polymer was mixed with three drops of microscope glue (Entellan PB 5265, Euromex Microscopes, Holland). Then, the mixture was transferred to the fresh surface of the pyrolytic graphite slide (NT-MDT comp.).

RESULTS AND DISCUSSION

The HIPEs consisted of a mixture of 1,3-DEB (10 and 20 vol % of the whole emulsion volume) as a monomer and sorbitane monooleate (Span80; 23 vol % according to the monomer) as a surfactant. The internal (droplet) phase used was pure deionized water (90 and 80 vol % of the whole emulsion volume) (*cf.* Scheme 1 and Supporting Information, Table S1). A ratio between the continuous and the internal phase allowed, after the polymerization of the continuous phase of the HIPE, the preparation of polyHIPE foams with 90% (sample ES117) and 80% (sample ES119) porosity. All HIPEs were stirred for 1 h at 400 rpm and afterward, the initiator [Rh(nbd)acac] complex (1 mol % with respect to the monomer dissolved in dichloromethane) was added (*cf.* Supporting Information, Table S1). Curing the HIPEs at room temperature resulted

Scheme 1. Preparation Protocol of the π -Conjugated PolyHIPE Foams with Intrinsic Porosity



in solid polymeric materials, which were purified by decantation in dichloromethane, filtered, and dried under vacuum at room temperature until they reached a constant weight. All the prepared polymers were brown-red brittle monolithic pieces, insoluble and nonswellable in tested solvents (THF, CH₂Cl₂, CHCl₃, and benzene). Before the determination of polymerization yields, a few milligrams of each polymer was suspended in THF for 5 h at room temperature and the liquid phase (filtered off) analyzed by SEC (a column used was suitable for the oligomeric molecular-weight (MW) range). The chromatograms of the THF extracts of both ES117 and ES119 samples show the absence of the low MW compound(s) as well as the soluble polymer. The polymerization yields, calculated gravimetrically by setting the mass of the dried monoliths in relation to the mass of the 1,3-DEB monomer, are 66 and 53% for the samples ES117 and ES119, respectively. The rigid monolithic pieces were further characterized by scanning electron microscopy (SEM) to visualize and evaluate the foam morphology. The typical open cellular polyHIPE architecture is observed for both samples (*cf.* Figure 1). The mean cavity diameter determined by the SEM image analysis¹⁸ (*cf.* Figure 1)

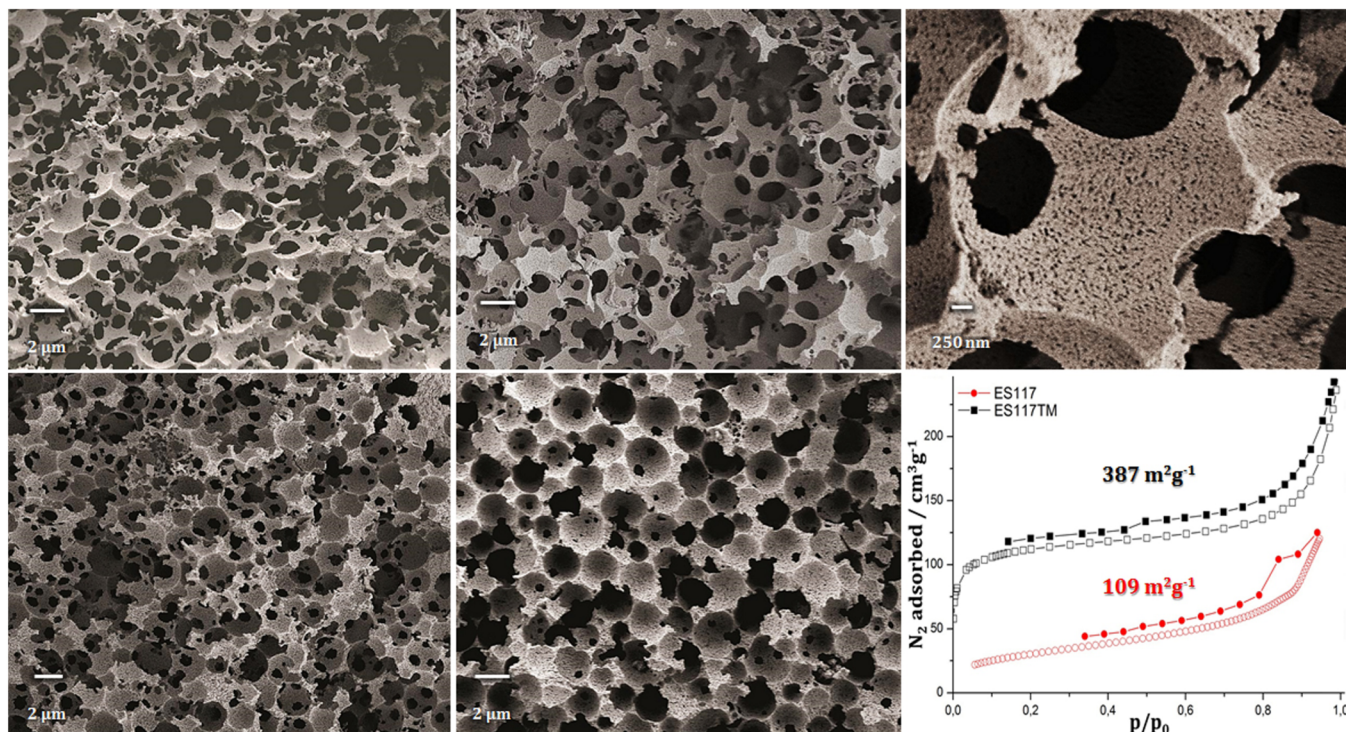


Figure 1. First row from left to right: SEM images of ES119, ES117, and ES117 at higher magnification. Second row from left to right: SEM images of samples ES119TM (upon thermal modification), ES119-CHOL (upon chemical modification with CHOL), and N₂ sorption isotherms (77 K) for samples ES117 (black squares) and ES117TM (red circles). Key: empty points, adsorption; full points, desorption.

is 4.8 ± 0.8 and $3.4 \pm 0.3 \mu\text{m}$ for the samples ES117 and ES119, respectively. The size of the interconnecting pores as determined from a mercury porosimetry data is 1.1 and $0.96 \mu\text{m}$ for the samples ES117 and ES119, respectively. The skeleton density as determined by a helium pycnometry is 1.21 and 1.17 g cm^{-3} for the samples ES117 and ES119, respectively (cf. Supporting Information Table S1). Of particular interest is the specific surface area of the novel polyacetylene-type π -conjugated polyHIPE foams. Generally, the polyHIPE foams prepared by polymerization of the HIPE emulsions tend to have rather low BET (Brunauer–Emmett–Teller) surface area (typically between 10 – $20 \text{ m}^2 \text{ g}^{-1}$) due to low the amount of micro/mesopores, and only upon their additional treatment by hypercross-linking¹⁹ or addition of inert porogens,²⁰ the surface area can be increased. In our case, an increase of the BET surface area from 15 (sample ES119) to $109 \text{ m}^2 \text{ g}^{-1}$ (sample ES117) can be ascribed to a syneresis effect, where the volume of CH_2Cl_2 used to dissolve the catalyst plays a role. Continuously growing polymer network inside discrete monomer-swollen micelles starts to precipitate in the form of gel-like nuclei that continue to grow and aggregate into the clusters through the process called syneresis.²¹ Micro/mesopores are then formed as spaces inside these precipitated polymeric clusters. In order to prevent collapsing of polymeric clusters during drying, the polymer phase has to be sufficiently rigid. In our case, the rigidity of the polymer is provided by the polyene character of the main chains and the high extent of cross-linking. The presence of micro/mesopores in ES117 can be deduced from the shape of N₂ adsorption isotherms (cf. Figure 1 and S4). Moreover, the highly magnified SEM image (cf. Figure 1) shows small macropores (size between 70 and 100 nm) within the walls of cavities, which were formed as

spaces between agglomerated polymeric clusters that precipitate during syneresis.

In addition, the specific surface area was further increased by applying the so-called solid-state hyper-cross-linking approach, which is, as compared to the solution based hyper-cross-linking,¹⁹ a solvent free approach that does not require a solvent to swell the polymer skeleton or a catalyst to trigger the postpolymerization cross-linking. In our approach, the remaining pendant ethynyl groups of the poly(1,3-DEB) skeleton were thermally reacted via the aromatization at 280°C .²² The thermally modified samples were labeled as ES117TM and ES119TM. The enlargement of the specific BET surface area from 15 to up to $184 \text{ m}^2 \text{ g}^{-1}$ for the sample ES119TM and from 109 to up to $387 \text{ m}^2 \text{ g}^{-1}$ for the sample ES117TM was observed from the data of nitrogen adsorption measurements (cf. Figure 1 and Supporting Information: Table S1 and Figure S4). After thermal modification an increase of skeletal density from 1.21 to 1.30 g cm^{-3} for the sample ES117 and from 1.17 to 1.36 g cm^{-3} for the sample ES119 was observed that reflects certain degree of hyper-cross-linking in the course of aromatization reaction. On the other hand, the macroporous architecture of the materials is totally preserved as indicate the SEM images of the thermally treated samples (cf. Figure 1 and Supporting Information Figure S3).

The chemical characterization of the newly obtained π -conjugated polyHIPEs comprised elemental analysis (EA), Fourier transform IR (FTIR), diffuse reflectance UV-vis (DR UV-vis) and photoluminescence (PL) spectroscopies as well as solid-state NMR spectroscopy (¹³C CP/MAS NMR). Examination of the elemental composition of the ES119 sample gave the values of 90.96% C and 4.52% H that result in an empirical formula of $\text{C}_{10}\text{H}_{5.9}$ (C_{10}H_6 theoretically) and a C/H molar ratio of 1.677 (1.667 theoretically). The EA of the thermally

modified ES119TM sample revealed the values of 86.72% C and 3.77% H that result in the empirical formula of $C_{10}H_{5.2}$ and the C/H molar ratio of 1.917 (cf. Supporting Information, Table S3). The increase in C/H molar ratio is ascribed to aromatization of the sample in the course of thermal modification. The same can be concluded from the EA results of the sample pair ES117 and ES117TM (Supporting Information, Table S3). The ^{13}C CP/MAS NMR spectra of the ES117 and ES119 samples show a broad, partly resolved signal in the region 115–150 ppm that corresponds to the aromatic carbons and the carbons of the polyene main chains,²³ while the signals at about 83 and 76 ppm are due to the carbons of the nonreacted pendant ethynyl groups (cf. Figure 2).⁸ The

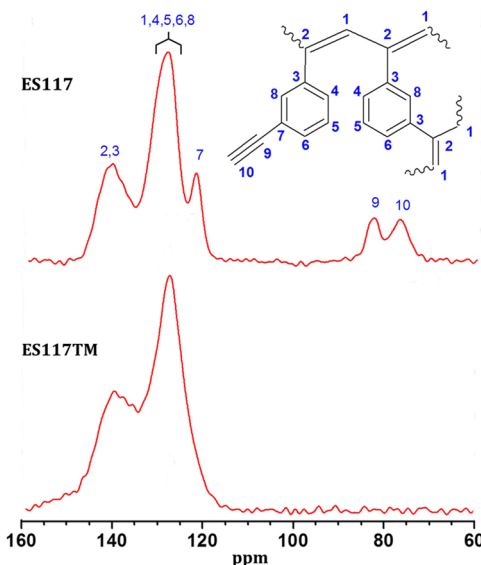


Figure 2. Enlarged ^{13}C CP/MAS NMR spectra of pristine ES117 (above) and thermally modified ES117TM (below) samples.

evaluation of the amount of free ethynyl groups from the ^{13}C CP/MAS NMR spectra of the ES117 and ES119 samples reveals the presence of about 5.1 mmol (ethynyl groups)/g, i.e. 0.64 of free ethynyl groups per one monomeric unit. Consequently, the degree of branching (DB) defined as DB

$= n_B/(n_L + n_B)$, where the n_B and n_L stand for the amounts of branched and linear monomeric units in polymer, respectively, is estimated to be 0.36 for both samples. In the ^{13}C CP/MAS NMR spectra of thermally modified ES117TM and ES119TM samples, no signals are observed in the region 76–83 and, thus, these results indicate complete or almost complete thermal transformation of the pendant ethynyl groups in parent samples (cf. Figure 2). The same conclusion results from the FTIR spectra of the thermally modified samples which particularly show an almost complete disappearance of the band at 3300 cm^{-1} ($\nu_{\equiv\text{C}-\text{H}}$) upon thermal modification of parent polymers (cf. Supporting Information: Figures S5 and S6). Because of fully conjugated nature of the polymer backbone, the DR UV-vis spectroscopy was performed and the spectra of both samples show a broad absorption band with the maximum in the region from 370 to 420 nm (cf. Figure 3). Upon samples' thermal modification the vis band tail red-shifted due to the enhanced extent of samples' conjugation (cf. Figure 3). When excited by the light of 420 nm wavelength both the parent and the thermally modified polymers exhibit photoluminescence manifested by a broad photoluminescence (PL) emission band with the maximum at 525 nm (parent polymers) and 530 nm (thermally modified polymers) (cf. Figure 3). Another way to postmodify the poly(1,3-DEB) backbone involved alkyne–azide cycloaddition (“click”) reaction via the nonreacted pendant ethynyl groups. Mimicking a biological surface within the synthetic 3D scaffolds is an attractive prospect to prepare porous polymers as potential scaffolds for cell culturing.²⁴ For this purpose the 1-azido-2,3,4,6-tetra-O-acetyl- β -D-glucose (GLU) and the 3 β -azido-5-cholestene (CHOL) were synthesized in accordance with the known synthetic procedure²⁵ and reacted with the remaining ethynyl groups of ES119 sample (cf. Scheme 2). A content of the GLU units in the ES119-GLU sample is 0.35 mmol/g and that of the CHOL units in the ES119-CHOL sample is 0.15 mmol/g as calculated based on the nitrogen content in the modified samples (see details in Supporting Information). Again, the polyHIPE architecture of chemically modified polymeric foams is totally preserved as reveal the SEM images of the ES119-GLU and ES119-CHOL samples (cf. Figure 1 and Supporting Information).

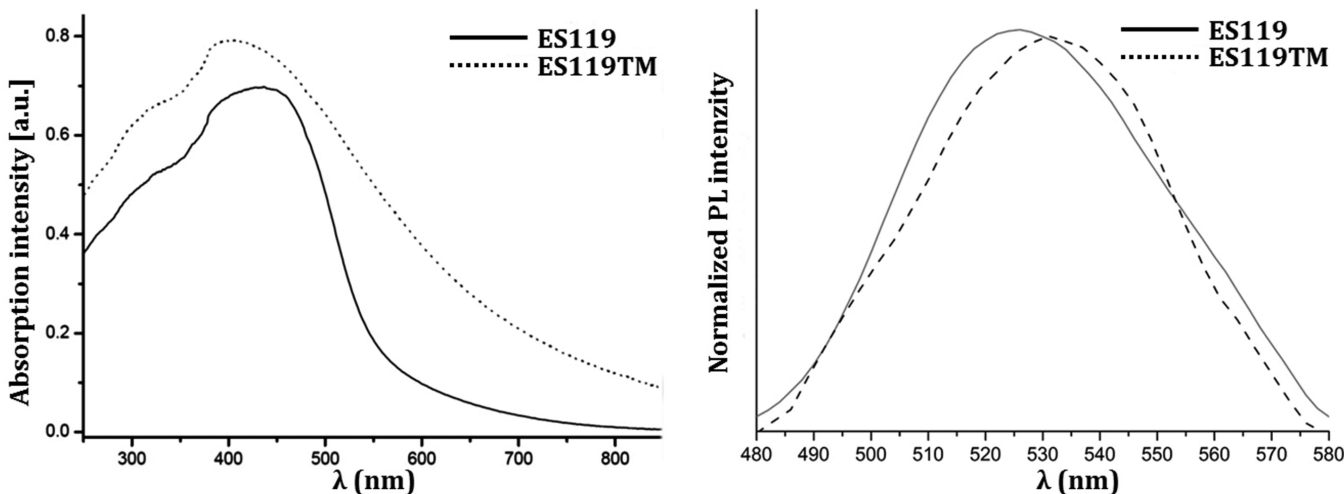
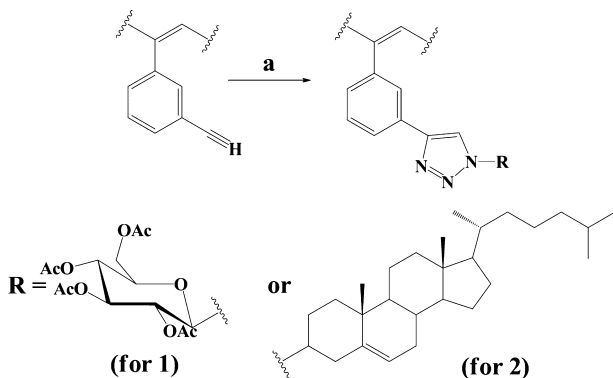


Figure 3. DR UV-vis spectra of pristine ES119 and thermally modified ES119TM samples (left) and photoluminescence (PL) spectra of pristine ES119 and thermally modified ES119TM samples (right).

Scheme 2. Chemical Modification Reactions: RN_3 , Heating in (a) Toluene (for 1) or Xylene (for 2)



CONCLUSIONS

The chain-growth, rhodium catalyzed, insertion polymerization was applied for the preparation of fully conjugated and reactive polyacetylene-type polyHIPE foams with intrinsic micro-porosity. Thus, obtained polymeric foams show well-defined hierarchically structured micro/macroporous polyHIPE architecture with significantly higher specific surface area as compared to the standard polyHIPE foams, and high inherent reactivity. Latter was demonstrated by alkyne–azide cyclo-addition of D-glucose azide and cholesteryl azide to the pendant ethynyl groups of the 1,3-DEB skeleton and by the solid phase hyper-cross-linking reaction. Chain-growth catalytic insertion polymerization (CIP) technique to solidify HIPEs can endow polyHIPE foams with unique electronic structure and properties that are very difficult to access with the corresponding vinyl monomers. Therefore, this chain-growth CIP has a great potential to extend the fields of advanced applications of this class of porous polymers in the future.

ASSOCIATED CONTENT

Supporting Information

Experimental details and additional SEM images, FTIR spectra, and N_2 sorption isotherm data. This material is available free of charge via the Internet at <http://pubs.acs.org>.

AUTHOR INFORMATION

Corresponding Authors

*(J.S.) E-mail: jan.sedlacek@natur.cuni.cz.
*(S.K.) E-mail: sebastijan.kovacic@ki.si.

Notes

The authors declare no competing financial interest.

ACKNOWLEDGMENTS

The authors gratefully acknowledge the financial support of the Ministry of Higher Education, Science and Technology of the Republic of Slovenia, the Slovenian Research Agency (Program P2-0145), the Czech Science Foundation (E.S., J.S., and J.Z., Projects No P108/11/1661), and the Science Foundation of the Charles University (E.S., Project No 580214). The authors thank Dr. J. Brus for NMR measurements, Dr. K. Jeřábek for texture characterization of polymers, and Mr. G. Kapun for SEM measurements.

REFERENCES

- (1) (a) Shiotsuki, M.; Sanda, F.; Masuda, T. *Polym. Chem.* **2011**, *2*, 1044. (b) Liu, J. Z.; Lam, J. W. Y.; Tang, B. Z. *Chem. Rev.* **2009**, *109*, 5799.
- (2) (a) Grimsdale, A. C.; Chan, K. L.; Martin, R. E.; Jokisz, P. G.; Holmes, A. B. *Chem. Rev.* **2009**, *109*, 897. (b) Jose, B. A. S.; Akai, K. *Polym. Chem.* **2013**, *4*, 5144. (c) Li, W.; Huang, H.; Lia, Y.; Deng, J. *Polym. Chem.* **2014**, *5*, 1107. (d) Sivkova, R.; Vohlídal, J.; Bláha, M.; Svoboda, J.; Sedláček, J.; Zedník, J. *Macromol. Chem. Phys.* **2012**, *213*, 411.
- (3) (a) Xu, Y.; Jin, S.; Xu, H.; Nagaia, A.; Juany, D. *Chem. Soc. Rev.* **2013**, *42*, 8012. (b) Liu, Q.; Tang, Z.; Wu, M.; Zhou, Z. *Polym. Int.* **2014**, *63*, 381.
- (4) McKeown, N. B.; Budd, P. M.; Msayib, K. J.; Ghanem, B. S.; Kingston, H. J.; Tattershall, C. E.; Makseid, S.; Reynolds, K. J.; Fritsch, D. *Chem.—Eur. J.* **2005**, *11*, 2610.
- (5) Dawson, R.; Ratvijitvech, T.; Corker, M.; Laybourn, A.; Khimyak, Y. Z.; Cooper, A. I.; Adams, D. J. *Polym. Chem.* **2012**, *3*, 2034.
- (6) (a) Palkovits, R.; Antonietti, M.; Kuhn, P.; Thomas, A.; Schuth, F. *Angew. Chem.* **2009**, *121*, 7042. (b) Dawson, R.; Adams, D. J.; Cooper, A. I. *Chem. Sci.* **2011**, *2*, 1173. (c) Stoeck, U.; Nickerl, G.; Burkhardt, U.; Senkovska, I.; Kaskel, S. *J. Am. Chem. Soc.* **2012**, *134*, 17335.
- (7) (a) Chen, Y.; Honsho, S.; Seki, I.; Jiang, D. *J. Am. Chem. Soc.* **2010**, *132*, 6742. (b) Brandt, J.; Schmidt, J.; Thomas, A.; Epping, J. D.; Weber, J. *Polym. Chem.* **2011**, *2*, 1950.
- (8) (a) Hanková, V.; Slováková, E.; Zedník, J.; Vohlídal, J.; Sivkova, R.; Balcar, H.; Zukal, A.; Brus, J.; Sedláček, J. *Macromol. Rapid Commun.* **2012**, *33*, 158. (b) Petrášová, S.; Zukal, A.; Brus, J.; Balcar, H.; Pastva, J.; Zedník, J.; Sedláček, J. *Macromol. Chem. Phys.* **2013**, *214*, 2856.
- (9) “polyHIPE” is a Unilever trademark.
- (10) Cameron, N. R.; Krajnc, P.; Silverstein, M. S. Colloidal Templating. In *Porous Polymers*; Silverstein, M. S., Cameron, N. R., Hillmyer, M. A. Eds.; Wiley & Sons: 2011.
- (11) Silverstein, M. S. *Prog. Polym. Sci.* **2014**, *39*, 199.
- (12) (a) Barbetta, A.; Dentini, M.; Leandri, L.; Ferraris, G.; Coletta, A.; Bernabei, M. *React. Funct. Polym.* **2009**, *69*, 724. (b) Audouin, F.; Fox, M.; Larragy, R.; Clarke, P.; Huang, J.; O’Connor, B.; Heise, A. *Macromolecules* **2012**, *45*, 6127–6135. (c) Wong, L. L. C.; Baiz Villafranca, P. M.; Menner, A.; Bismarck, A. *Langmuir* **2013**, *29*, 5952.
- (13) Lamson, M.; Epshtain-Assor, Y.; Silverstein, M. S.; Matyjaszewski, K. *Polymer* **2013**, *54*, 4480.
- (14) Luo, Y.; Wang, A.-N.; Gao, X. *Soft Matter* **2012**, *8*, 1824.
- (15) (a) Lovelady, E.; Kimmins, S. D.; Wu, J.; Cameron, N. R. *Polym. Chem.* **2011**, *2*, 559. (b) Sergent, B.; Birota, M.; Deleuze, H. *React. Funct. Polym.* **2012**, *72*, 962.
- (16) (a) Deleuze, H.; Faivre, R.; Herroguez, V. *Chem. Commun.* **2002**, 2822. (b) Kovačič, S.; Krajnc, P.; Slugovc, C. *Chem. Commun.* **2010**, *46*, 7504. (c) Kovačič, S.; Jeřábek, K.; Krajnc, P.; Slugovc, C. *Polym. Chem.* **2012**, *3*, 325. (d) Kovačič, S.; Matsko, N. B.; Jeřábek, K.; Krajnc, P.; Slugovc, C. *J. Mater. Chem. A* **2013**, *1*, 487. (e) Kovačič, S.; Kren, H.; Krajnc, P.; Koller, S.; Slugovc, C. *Macromol. Rapid Commun.* **2013**, *34*, 581. (f) Knall, A.-C.; Kovacic, S.; Hollauf, M.; Reishofer, D. P.; Saf, R.; Slugovc, C. *Chem. Commun.* **2013**, *49*, 7325. (g) Kovačič, S.; Matsko, N. B.; Ferk, G.; Slugovc, C. *J. Mater. Chem. A* **2013**, *1*, 7971. (h) Kovačič, S.; Preishuber-Pflugl, F.; Slugovc, C. *Macromol. Mater. Eng.* **2014**, *299*, 843.
- (17) (a) Zhang, K. A. I.; Vobecka, Z.; Tauer, K.; Antonietti, M.; Vilela, F. *Chem. Commun.* **2013**, *49*, 11158. (b) Wang, Z. J.; Landfester, K.; Zhang, K. A. I. *Polym. Chem.* **2014**, *5*, 3559.
- (18) Barbetta, A.; Cameron, N. R. *Macromolecules* **2004**, *37*, 3188.
- (19) (a) Schwab, M. G.; Senkovska, I.; Rose, M.; Klein, N.; Koch, M.; Pahnke, J.; Jonschker, G.; Schmitz, B.; Hirscher, M.; Kaskel, S. *Soft Matter* **2009**, *5*, 1055. (b) Pulko, I.; Wall, J.; Krajnc, P.; Cameron, N. R. *Chem.—Eur. J.* **2010**, *16*, 2350.
- (20) Barbetta, A.; Cameron, N. R. *Macromolecules* **2004**, *37*, 3202.

- (21) (a) Gokmen, M. T.; Du Perez, F. E. *Prog. Polym. Sci.* **2012**, *37*, 365. (b) Sterchele, S.; Centomo, P.; Zecca, M.; Hanková, L.; Jeřábek, K. *Microporous Mesoporous Mater.* **2014**, *185*, 26.
- (22) Tseng, W.-C.; Chen, Y.; Chang, G.-W. *Polym. Degrad. Stab.* **2009**, *94*, 2149.
- (23) Sedláček, J.; Vohlídal, J.; Cabioch, S.; Lavastre, O.; Dixneuf, P.; Balcar, H.; Štícha, M.; Pfleger, J.; Blechta, V. *Macromol. Chem. Phys.* **1998**, *199*, 155.
- (24) Hayward, A. S.; Eissa, A. M.; Maltman, D. J.; Sano, N.; Przyborski, S. A.; Cameron, N. R. *Biomacromolecules* **2013**, *14*, 4271.
- (25) (a) Kumar, R.; Maulik, P. R.; Misra, A. K. *Glycoconjugate J.* **2008**, *25*, 595. (b) Sun, Q.; Cai, S.; Peterson, B. R. *Org. Lett.* **2009**, *11*, 567.